

# The Free Energy, Enthalpy and Entropy of Native and of Partially Denatured Closed Circular DNA

William R. Bauer<sup>1</sup> and Craig J. Benham<sup>2</sup>

<sup>1</sup>Department of Microbiology, Health Sciences Center  
State University of New York  
Stony Brook, NY 11794-5222, U.S.A.

<sup>2</sup>Department of Biomathematical Sciences  
Box 1023, Mount Sinai School of Medicine  
1 Gustave Levy Place, New York, NY 10029, U.S.A.

(Received 12 April 1993; accepted 14 July 1993)

We have used gel electrophoresis to measure the progress of local denaturation in closed circular pBR322 DNA as a function of temperature and linking deficiency,  $\Delta Lk$ . Local denaturation is closely coupled to supercoiling in closed DNA, requiring statistical mechanical methods for analysis. We have applied these methods to the experimental data to evaluate the free energies for three associated molecular processes. These processes are changes in the residual linking deficiency,  $\Delta Lk_r$ , initiation of local denaturation, and twisting of denatured strands about one another. Our results confirm the quadratic dependence of the supercoiling free energy upon  $\Delta Lk$ , with a free energy coefficient of  $740/N$  kcal/mol at 37°C, where  $N$  is the number of base-pairs. The free energy of initiation of denaturation is  $10.2(\pm 0.7)$  kcal/mol. The free energy of interstrand twisting of denatured regions varies with the square of the twist density, with proportionality coefficient  $C_t = 1.62(\pm 0.11)$  kcal/rad<sup>2</sup> at 37°C. We have also calculated the entropy and enthalpy of these three processes, using the temperature dependence of the respective free energies. We find that both the entropy and the enthalpy of supercoiling are positive and vary quadratically with  $\Delta Lk$ . The free energy of initiation of denaturation is independent of temperature, hence arises primarily from a change in enthalpy. The entropy and enthalpy of interstrand twisting of denatured regions are both positive, and the twisting force constant decreases with temperature. These results differ considerably from expectations based solely upon considerations of chain configuration *in vacuo*, indicating the importance of solvent-dependent factors in determining the structure of closed circular DNA.

**Keywords:** closed circular DNA; gel electrophoresis; thermodynamics of super coiling; DNA denaturation

## 1. Introduction

The physical and chemical properties of closed circular DNA are significantly changed by the linking of the two covalent continuous strands. Its biological interactions are also profoundly affected, including protein and other ligand binding, transcription, replication, recombination, and many others (Bauer, 1978; Bauer & Gallo, 1989). These altered functions can be divided into those associated either with the molecule's secondary or with its tertiary structure. The former category includes changes in the helical repeat (White *et al.*, 1988), torsional tension on the duplex (Sinden *et al.*, 1980; Sinden & Pettijohn, 1982), transitions from one duplex structural form to another (Klysik *et al.*,

1991; Lilley, 1987; Nordheim *et al.*, 1982), and changes in chemical reactivity (Bauer & Gallo, 1989). The tertiary structure category includes phenomena such as loop formation (Lobell & Schleif, 1990; Schleif, 1988), compaction (Adrian *et al.*, 1990; Boles *et al.*, 1990), and juxtaposition of distant segments in recombination (Benjamin & Cozzarelli, 1985; Bliska & Cozzarelli, 1987).

The division into secondary and tertiary structural factors is reflected in the basic conservation law (White, 1969):

$$Lk = \text{constant} = Tw + Wr. \quad (1)$$

The linking number,  $Lk$ , is the conserved topological property. The twist,  $Tw$ , is the geometric

factor associated with secondary structure; and the writhe,  $Wr$ , is a geometric factor associated with tertiary structure. A detailed exposition of the technical definitions and methods of calculation of these three quantities has been presented (White, 1989). An important associated quantity for describing closed circular DNA is its linking deficiency,  $\Delta Lk$ , defined by:

$$\Delta Lk = Lk - Lk_0, \quad (2)$$

where  $Lk_0 = N/h_0$ ,  $N$  is the number of base-pairs in the DNA, and  $h_0$  is the helical repeat of linear DNA, 10.5 bp/turn in NaCl (Rhodes & Klug, 1980; Wang, 1979). Distinct topoisomers differ only in  $\Delta Lk$ . In the experiments analyzed here and in most biological contexts the population average value of the linking difference,  $\langle \Delta Lk \rangle$ , is negative.

Closed circular DNA is also characterized by its own set of energy relationships. These are expressed in terms of the thermodynamic state functions,  $\Delta G$ ,  $\Delta H$  and  $\Delta S$ , associated with structural changes and chemical reactivity. A more detailed description of the state of the DNA also includes the mechanical force constants, the torsional rigidity and the bending modulus, that determine the displacement response to applied forces. When conditions favor a change in duplex structure, this process is characterized by its own thermodynamic and mechanical energy functions. Local denaturation is strongly influenced by the topological constraint in closed DNA, a situation that differs profoundly from that in linear or nicked circular DNA. Generally speaking, local denaturation takes place at lower temperatures as the linking number deficit increases. This phenomenon was recognized quite early (Vinograd & Lebowitz, 1966).

In the research described here, we determine the thermodynamic properties of closed circular DNA from measurements of the change in electrophoretic mobility of its topoisomers as a function of temperature and  $\Delta Lk$ . These experiments are designed to take advantage of our earlier finding that local duplex unwinding can be initiated either by an increase in temperature or by a reduction in the linking number (Lee & Bauer, 1985). Normally, an increase in  $|\Delta Lk|$  brings about compaction as the DNA increasingly supercoils, hence the mobility increases with increasing  $|\Delta Lk|$ . In the event that increasing  $|\Delta Lk|$  triggers local duplex unwinding, however, superhelical strain is relieved and the supercoiled structure becomes temporarily more extended. The associated reduction in mobility reflects the occurrence of duplex unwinding. It is now known (Kowalski *et al.*, 1988) that, for pBR322 DNA at low salt concentration and 37°C, the duplex unwinding is entirely local denaturation and not cruciform extrusion or any other type of unwinding transition (refer to Discussion).

The residual linking deficiency,  $\Delta Lk_r$ , which is that portion of  $\Delta Lk$  not accounted for by either duplex unwinding or by rotational deformations of the denatured regions, is determined from the relative reduction in electrophoretic mobility of

partially denatured topoisomers. For a non-denatured closed circular DNA,  $\Delta Lk_r = \Delta Lk$ . As denaturation proceeds,  $\Delta Lk_r$  deviates increasingly from  $\Delta Lk$ . We employ methods of statistical mechanics to interpret changes in  $\Delta Lk_r$  in terms of the extent of the associated denaturation and the coupled change in the extent of supercoiling. The methods have been developed previously (Benham, 1990, 1992) and were used successfully to analyze local denaturation in closed circular pBR322 DNA at low salt and a single temperature (37°C; Kowalski *et al.*, 1988). These calculations determine the energies of the various transitions in closed circular DNA that are required to bring about the observed transfer of linking deficiency from  $\Delta Lk$  to  $\Delta Lk_r$ . In the present research, the same techniques are used to calculate the free energies that characterize both native and partially denatured closed circular pBR322 DNA at several temperatures. From the temperature dependence of these free energies, we find the enthalpy and entropy associated with supercoiling and with denaturation in closed circular DNA.

Our independent estimate of the topological constraint (supercoiling) free energy agrees well with previous determinations, when our results are extrapolated to temperatures of 37°C or below. The supercoiling enthalpy is positive and agrees in magnitude with the available calorimetric data (Seidl & Hinz, 1984). We find that the entropy contribution to the supercoiling free energy is positive and is roughly half the magnitude of the enthalpy. This means that an increase in temperature reduces the unfavorable free energy of supercoiling.

It is useful to compare our experimental result for the entropy with Monte Carlo calculations of the chain configuration entropy for closed circular DNA (Vologodskii *et al.*, 1992). These latter theoretical calculations predicted a negative entropy change that varies non-quadratically with  $\Delta Lk$ . In contrast, the present experiments find a positive entropy change that varies quadratically with  $\Delta Lk$ . These major differences lend emphasis to the importance of non-chain configuration factors for a complete description of the energetics of closed circular DNA. Such factors include solvent-DNA interactions, solvent structure changes, and entropy and enthalpy effects that arise from changing local interactions as the linking difference is varied. It is clear that, although *in vacuo* chain statistical calculations are instructive from a theoretical point of view, great caution must be exercised in using them to predict the solution properties of closed circular DNA.

We also obtain the thermodynamic functions for the initiation of local melting in closed circular DNA. Our estimate of the free energy of initiation of denaturation, 10.22 ( $\pm 0.67$ ) kcal/mol, agrees with earlier results using pBR322 DNA at 37°C (Benham, 1992). The initiation free energy may be interpreted as the sum of a base stacking factor and a loop entropy factor. When allowance is made for

the latter, we estimate that the stacking contribution to the initiation free energy is approximately 7 kcal/mol, comparable to earlier determinations involving linear DNA molecules (Amirikyan *et al.*, 1981; Crothers & Zimm, 1964). Because of the net torsional tension in closed circular DNA of reduced  $\Delta Lk$ , a denatured region engages in non-base-paired left-handed winding. We estimate the force constant for this winding to be  $1.3 \times 10^{-13}$  erg/rad<sup>2</sup> (1.87 kcal/rad<sup>2</sup>) at 30°C. The entropy change associated with the left-handed winding of a denatured region is also positive, pointing out the likely importance of solvent effects in this process as well.

## 2. Experimental Methods

### (a) DNA and topoisomer preparation

pBR322 DNA was prepared and purified by standard methods (Sambrook *et al.*, 1989). Following purification the DNA was ethanol-precipitated and resuspended in topoisomerase relaxation buffer (20 mM Tris (pH 8.1), 200 mM KCl, 0.5 mM DTT, 0.1 mM EDTA, 30  $\mu$ g/ml bovine serum albumin). Extended families of topoisomers were prepared from a stock of high initial superhelix density, obtained by the addition of EtdBr to a concentration of 2 to 3  $\mu$ g/ml and incubation at 37°C with calf thymus type I topoisomerase (Sigma). The reaction was stopped by phenol-extraction (2 $\times$ ), followed by ethanol-precipitation. The resuspended plasmid DNA of high superhelix density (0.2  $\mu$ g in 25  $\mu$ l) was then treated for 30 min on ice with topoisomerase I (1.0 unit), and the reaction was stopped by the addition of 6.25  $\mu$ l of 5% (w/v) SDS, 0.15% (w/v) bromophenol blue, 50% (v/v) glycerol, 10 mM Tris (pH 8.0), 1 mM EDTA. The solution was preincubated for 10 min at the temperature of the first gel, then layered.

### (b) Gel electrophoresis

First-dimension gel electrophoresis employed an insulated, thermostated cylindrical Buchler apparatus maintained at constant temperature with a Lauda model B-2 circulator. Agarose tube gels, 0.7% (w/v), were prepared in E-buffer (90 mM Tris-borate (pH 8.4 at 25°C)) in 27 cm  $\times$  0.6 cm (id) glass tubes, then cut to a standard length of 22 cm. Electrophoresis was conducted at 45 V for 18 h, following which the cylindrical gel was removed and sliced to a 12.5 cm length containing the topoisomers. This segment was placed in a 13 cm  $\times$  0.6 cm  $\times$  0.7 cm (deep) well at one end of a 15 cm  $\times$  15 cm  $\times$  0.8 cm horizontal slab gel (0.7% agarose in E buffer containing chloroquine phosphate). Second-dimension electrophoresis was at 55 V for 18 h at 25°C. Staining, gel photography and other procedures were as described previously (Lee & Bauer, 1985). All first-dimension gel electrophoresis experiments were conducted under the same conditions, hence the electrophoretic mobilities are directly proportional to the distances migrated. Relative mobilities at each temperature were calculated as the ratio of distance migrated for a given topoisomer to the distance migrated for the topoisomer nearest to  $\Delta Lk = 0$ .

### (c) Measurement of gels and calculations

The second-dimension gel was photographed with Polaroid film and scanned with a UMAX model UC630 scanner. An image of the negative was produced with

Adobe Photoshop, running on a Macintosh Quadra 950. The locations of the topoisomers were measured on this scanned image with the program Image 1.45 (NIH).

The principal uncertainty in the determination of the residual linking differences arises in finding the  $\Delta Lk$  value corresponding to the onset of denaturation. The topoisomer with the largest mobility may actually undergo partial denaturation, even though the resulting retardation is insufficient to permit other topoisomers to pass it on the gel. Because mobilities are the same for undenatured topoisomers of the same  $|\Delta Lk|$ , regardless of sign, the fractional relaxation of the fastest negative topoisomer was interpolated from the positions of the corresponding positively supercoiled topoisomers if bracketing positive topoisomers were present. If these were not available, the differences between the migration distances of neighbor pairs of undenatured negative topoisomers were determined. This procedure resulted in a list of migration distances as a function of  $\Delta Lk$ . Extrapolation to the  $\Delta Lk$  of the fastest topoisomer permitted estimation of its expected migration distance in the absence of denaturation. Comparison of this value to its actual distance migrated provided an estimate of the extent of denaturation of this topoisomer. A more detailed description of the measurement techniques was provided previously (Lee & Bauer, 1985).

## 3. Theoretical Analysis

### (a) Analytic methods

The linking difference,  $\Delta Lk$ , of a particular topoisomer can be partitioned in various ways, of which three are important in the present context. First, local regions of the molecule may denature. This transfers base-pairs having the torsionally unstressed winding of B-DNA to pairs of monomer units lacking hydrogen bonds and having no net interstrand twist. The free energy of local denaturation,  $\Delta G_{den}$ , is positive under conditions in which the most stable DNA structure is the duplex. Second, the separated strands in these denatured regions may twist. The single strands in a denatured region are more flexible than the relatively stiff duplex (Hagerman, 1988; Manning, 1988), and they are no longer subject to the strict spatial requirements imposed by base-pairing. This means that they can twist around each other, normally in a left-handed sense. When local denaturation occurs in a topoisomer of negative  $\Delta Lk$ , some of this linking difference can be accommodated by these twist reductions. Third, the balance of the  $\Delta Lk$ , which remains associated with the molecule as a whole, is termed the residual linking difference, or  $\Delta Lk_r$ . In the absence of denaturation, the entire linking difference,  $\Delta Lk$ , stresses the molecule; whereas in a partially denatured molecule the magnitude of the global deformation is reduced to  $\Delta Lk_r$ . The equilibrium favors denaturation when the resulting reduction in global deformation strain energy exceeds the energy cost of local denaturation, including unstacking, breaking of hydrogen bonds, interstrand twisting of denatured regions, etc.

The complete theory for the analysis of local structural transitions in closed circular DNA has been derived previously (Benham, 1990, 1992), and

reference should be made to those publications for the details of the calculations. The approach is to use statistical mechanics to calculate ensemble averages of the quantities of interest over all microstates of the closed circular DNA. There are, for example,  $2^N$  microstates for a plasmid DNA molecule containing a run of  $N$  base-pairs subject to denaturation. The individual microstates become less densely occupied exponentially as their free energies increase. For purposes of designing the computer calculations, all low-energy microstates are found exactly, and the high-energy microstates (those occupied with very low frequency) are treated collectively. Quantities whose ensemble average values are computed include the probability of separation at each base-pair in the DNA, the number of separated base-pairs, the number of these that are A·T, and the residual linking difference. We emphasize that these calculated quantities are dependent variables, not adjustable parameters. Their values are determined by solution of the statistical mechanical equations, subject to the initial and boundary conditions.

Under conditions in which local denaturation is favored, the total free energy of a closed circular DNA is derived from three sources. The first of these is the free energy associated with the initiation ( $a$ ) and continuation ( $b$ ) of the denaturation transition,  $\Delta G_{\text{den}}(a, b)$ . The second is the free energy required for interstrand winding of the two single strands within a separated region,  $\Delta G(\tau)$ . The third is the free energy associated with supercoiling deformations of the DNA having a defined residual superhelix density,  $\sigma_r$  (see below),  $\Delta G(\sigma_r)$ . The energy considerations governing these three types of deformations are described separately in the following sections. The total free energy of a state  $i$  is the sum of the contributions from these three factors:  $\Delta G_i = \Delta G_{\text{den}}(a, b) + \Delta G(\tau) + \Delta G(\sigma_r)$ . The partition function of the system is then:

$$Z = \sum_i e^{-\Delta G_i/RT},$$

and the fractional occupancy of state  $i$  at equilibrium is:

$$p_i = \frac{e^{-\Delta G_i/RT}}{Z}.$$

If any quantity  $x$  has value  $x_i$  in state  $i$ , then its population average value at equilibrium is:

$$\langle x \rangle = \sum_i x_i p_i.$$

#### (b) The energetics of local denaturation

The free energy of denaturation (strand separation),  $\Delta G_{\text{den}}(a, b)$ , is divided into two contributions. First, an initiation free energy  $a$  is needed to begin the formation of a run of denatured base-pairs. This energy is required to form the pair of junctions between the local strand-separated region and the adjoining duplex regions, and to accommodate the

altered conformational states accessible to the separated region. Separation of the initial base-pair requires that two stacking interactions be disrupted, one with the adjoining base-pair on each side. Each extension of the run of separated base-pairs, in contrast, disrupts stacking only on one side. The available experimental evidence indicates that the initiation free energy  $a$  is quite large, and estimates in the range 10 to 12 kcal/mol have been reported (Amirikyan *et al.*, 1981; Benham, 1992). The size of this term means that strand separation in closed circular DNA is a highly competitive transition; consequently, the lowest energy states of partially denatured, closed circular DNA contain one or only a few distinct regions of strand separation. In the present treatment, the parameter  $a$  is regarded as an unknown quantity, to be determined by fitting to experimental data. We assume that the initiation free energy,  $a$ , is the same at all transition sites. While this free energy might in principle show some sequence dependence, the major contributions (disrupting stacking, forming junctions, and altering the configuration) are shared by all separated regions. For this reason, any dependence of this term upon base sequence is expected to be small.

The second energy component of strand separation is the incremental free energy of separating each base-pair in a denatured region,  $b$ . This term depends primarily on the identity of the base-pair involved, and secondarily on the identities of its neighbors. In general, the free energy of disrupting an A·T base-pair is less than that needed to separate a G·C pair. The free energy  $b_j$  needed to separate base-pair  $j$  is given by:

$$b_j = \Delta H_j \left( 1 - \frac{T}{T_m} \right), \quad (3)$$

where  $\Delta H_j$  is the enthalpy of transition and  $T_m$  is the transition temperature for separation.  $T_m$  depends on sequence and monovalent cation concentration  $x$  according to (Marmur & Doty, 1962; Schildkraut & Lifson, 1965):

$$T_m = 354.55 + 16.6 \log(x) + 41f_{GC}, \quad (4)$$

where  $f_{GC}$  is the mole fraction of G·C base-pairs.

We have allowed  $\Delta H_j$  to take one average value for A·T base-pairs and another average value for G·C base-pairs. These averages weight the contributions from nearest neighbors according to the probability of occurrence of each type as determined from the base composition. For pBR322 DNA, we take the average enthalpies of transition to be 7.25 kcal/mol for A·T base-pairs and 9.02 kcal/mol for G·C pairs, as determined from sequence-dependent calorimetric measurements (Breslauer *et al.*, 1986). Sample calculations have shown that the use of exact nearest neighbor enthalpies does not significantly modify the transition energies,  $b_j$ . This is because the calculations of the thermodynamic state

changes are independent of the mechanism of the transition itself (the path) and require only the initial (duplex) and final (melted) states. Because denaturation occurs in the immediate vicinity of the corresponding  $T_m$ , the factor  $(1 - T/T_m)$  in equation (3) reduces the effects of nearest neighbor variations in  $\Delta H_j$  by at least an order of magnitude. This would change the  $b_j$  for any individual base-pair by less than 0.1 kcal/mol from the value used here, with these alterations tending to average out over a run of separated base-pairs. Extensive sample calculations have shown that changes on this scale have a negligible influence on the computed equilibria. Values of the parameter  $b$  for G·C and for A·T base-pairs are regarded as known in the present analysis, and no independent values were determined.

The total free energy required to create  $r$  runs of strand separation, the  $i$ th of which contains  $n_i$  specific bases, is:

$$\Delta G_{\text{den}}(a, b) = \sum_{i=1}^r \left( a_i + \sum_{j=1}^{n_i} b_{ij} \right). \quad (5)$$

Here  $b_{ij}$  is the free energy of separating the  $j$ th base-pair in the  $i$ th run, while  $a_i$  is the initiation free energy for the  $i$ th run.

#### (c) The energetics of topologically constrained DNA

The free energy of closed circular DNA has been shown by dye binding experiments to vary approximately quadratically with  $\Delta Lk$  over a wide range of linking differences (Bauer & Vinograd, 1970):

$$\Delta G(\Delta Lk) = K(\Delta Lk)^2. \quad (6a)$$

This free energy was originally termed the free energy of superhelix formation (Bauer & Vinograd, 1970). However, it is associated not with the geometric but with the topological state of the DNA. For this reason, we prefer the designation topological constraint free energy (or supercoiling free energy, as a less formal alternative). In previous theoretical work the constant  $K$  in equation (6a) was introduced as  $K/2$ , consistent with its origin in a Taylor series expansion. In the present treatment we adopt a definition of  $K$ , lacking the factor of 2, that accords with most other reports in the literature. The topological constraint free energy is more generally written in terms of the specific linking difference,  $\sigma = \Delta Lk/Lk_0$ , as:

$$\Delta G(\sigma, T) = K Lk_0^2 \sigma^2, \quad (6b)$$

where the temperature dependence of  $K$  has been explicitly recognized. The coefficient  $K$  for a molecule containing  $N$  base-pairs is given by

$$K = \frac{RTq(T)}{N}. \quad (6c)$$

When the results of Bauer & Vinograd (1970) are recalculated to account for the correct dye binding angle, their measured quadratic coefficient becomes

$q = 985$  at high salt concentration (5.6 M CsCl). The coefficient  $q$  has also been evaluated from the measured variance in an equilibrium Boltzmann distribution of topoisomers around the relaxed state (Depew & Wang, 1975; Pulleyblank *et al.*, 1975), referred to as the Gaussian center method. These latter experiments were conducted at electrophoresis salt concentrations (approximately 25 mM), employing closed circular DNAs of various origins, and yielded the average result  $q = 1100$ . This coefficient also has been estimated, from the early denaturation of pBR322 DNA at 10 mM NaCl, 37°C, to be  $q = 1175$  (Benham, 1992). The average value obtained for all DNAs of length >2400 bp is  $q = 1115$  (Bauer & Gallo, 1989), at temperatures of 37°C or less.

In the analytic methods used here, the free energy of a closed circular DNA is calculated from the residual linking difference  $\Delta Lk_r$ , which is that portion of the initial linking difference  $\Delta Lk$  that is not accommodated either by local strand separation (the local unwinding of the B-DNA duplex) or by subsequent interstrand twisting in the denatured regions. In states where no denaturation occurs,  $\Delta Lk_r = \Delta Lk$ . The associated specific linking differences are designated  $\sigma_r$  and  $\sigma$ , respectively. In a closed circular DNA containing a denatured region,  $\Delta G(\sigma)$  is calculated from equation (6b) and  $\sigma_r$ .

#### (d) The energetics of interstrand twisting of single strands

Because single-stranded DNA is relatively flexible, a substantial portion of  $\Delta Lk$  can be accommodated at a small energy cost by interstrand twisting of denatured regions. If there are  $n$  separated base-pairs in the denatured domain, each of which is twisted to a helicity of  $\tau$  radians, the free energy is:

$$\Delta G(\tau, T) = \frac{1}{2} C_\tau n \tau^2, \quad (7)$$

where  $C_\tau$  is the temperature-dependent force constant for interstrand winding of coiled regions.

The use of a simple harmonic expression for the free energy term in equation (7) follows from the boundary conditions. The free energy  $\Delta G(\tau)$  can, in general, be expressed by a power series in  $\tau$ . The two unpaired strands in a denatured region are physically free to assume random coil configurations in the absence of constraints, so that any interstrand rotation will constitute an entropy restriction that reduces  $\Delta S(\tau)$  and thereby increases  $\Delta G(\tau)$ . In consequence, the state of minimum free energy occurs in the interstrand untwisted condition,  $\tau = 0$ . This insures that the coefficients of the zero and first-order terms in  $\tau$  in the power series both vanish. The first non-zero term is thus the quadratic. Terms involving higher powers of  $\tau$  are neglected.

The force constant  $C_\tau$  is taken to be the same for all base-pairs. This is reasonable, because sequence effects are expected to average out over the region involved. The possible dependence of  $C_\tau$  upon base sequence cannot be addressed at present.

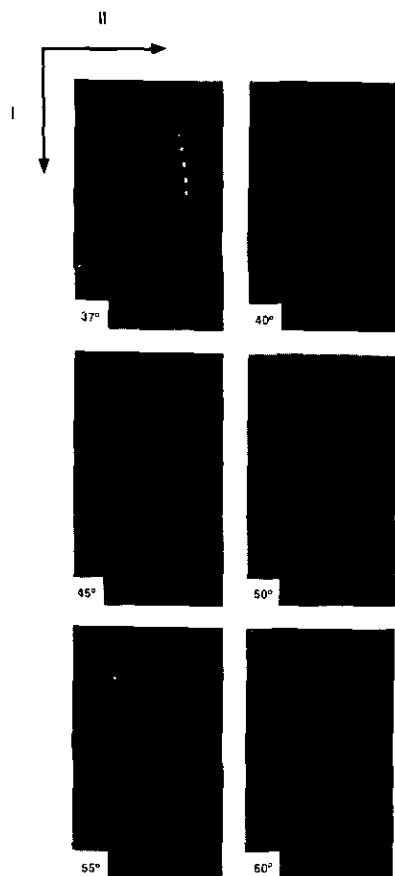


**Figure 1.** Gel electrophoresis analysis of topoisomer distributions at various temperatures. The first-dimension electrophoresis (not shown) took place in 22 cm glass tubes containing 0.7% agarose in E buffer, thermostated to the desired temperature in a Buchler apparatus. Following the second dimension of electrophoresis, the gels were stained with ethidium bromide and photographed (shown here). The isolated band in the upper left-hand corner of each photograph is nicked circular DNA. The direction of electrophoresis in each dimension is as indicated.

#### 4. Results

##### (a) Determination of the energy parameters

Two-dimension gel electrophoresis experiments were performed using pBR322 DNA at an ionic strength of 30 mM, at temperatures of 37°C to 60°C. Figure 1 shows the experimental results for all temperatures. The gels were analyzed as described above to determine the migration distances of the various topoisomers and the linking differences of each. The residual linking difference of each topoisomer experiencing retardation was determined by interpolation of its migration distance between those of the undenatured topoisomers of smaller  $|\Delta Lk|$ . Thus, denaturation of a run of  $n$  base-pairs leads to a decrease in duplex winding of  $n(1/h_0 - \tau/2\pi)$ . In consequence,  $\Delta Lk_r$  becomes more negative by the same amount. A numerically equal apparent shift in topoisomer number will be observed by gel electrophoresis.

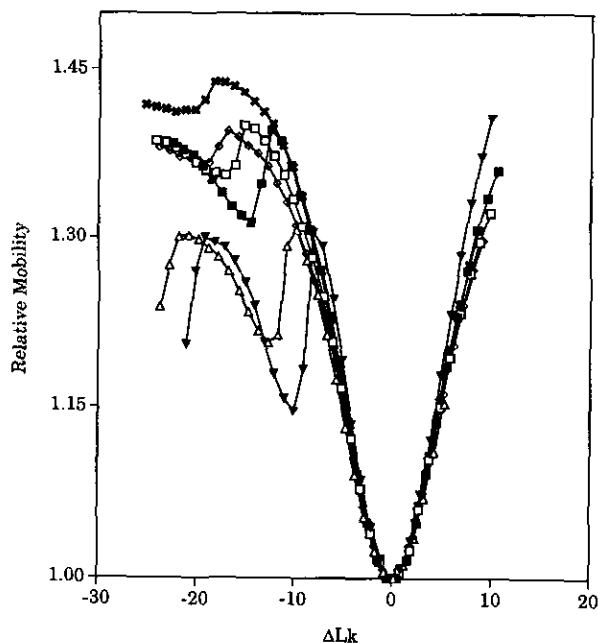


**Figure 2.** Plots of relative electrophoretic mobility versus  $\Delta Lk$  for pBR322 DNA at various dimension electrophoresis temperatures. The data were measured at first dimension temperatures of 37°C ( $\times$ ), 40°C ( $\diamond$ ), 45°C ( $\square$ ), 50°C ( $\blacksquare$ ), 55°C ( $\triangle$ ) and 60°C ( $\blacktriangledown$ ).

Figure 2 shows a plot of the relative mobilities as a function of linking difference for all topoisomers at all temperatures. For each temperature those topoisomers experiencing local denaturation were selected, together with the topoisomer immediately prior to the onset of denaturation. The other topoisomers of lower  $|\Delta Lk|$ , which showed no denaturation, were not used in the curve-fitting procedure. The transition behavior was analyzed for each temperature separately. However, the data at 37°C were not analyzed because the small retardations observed precluded the accurate determination of residual linking differences in this case.

Initial values of the three floating parameters  $q$ ,  $a$  and  $C_t$  were specified, and the theoretical transition behavior of each topoisomer was computed. The predicted  $\Delta Lk_r$  was found for each, and this set of values was used to calculate the root-mean-square (r.m.s.) deviation from the experimental data. New values of the floating parameters were then chosen, and this process was repeated. The  $(q, a, C_t)$  parameter space was sampled by first fixing a value of  $C_t$ , and varying the other two parameters  $a$  and  $q$  in a  $10 \times 12$  grid. Initially the spacing of this grid was chosen to be wide. This procedure was repeated using a coarse grid until the unique region was found where the goodness-of-fit was optimized. Then a finer grid was examined, centered in the region of this optimum. This procedure was repeated as needed until the values of  $a$  and  $q$  giving optimum fit for the given value of  $C_t$  were determined. In all cases a unique minimum of the r.m.s. deviation was found, so the fit procedure was unam-

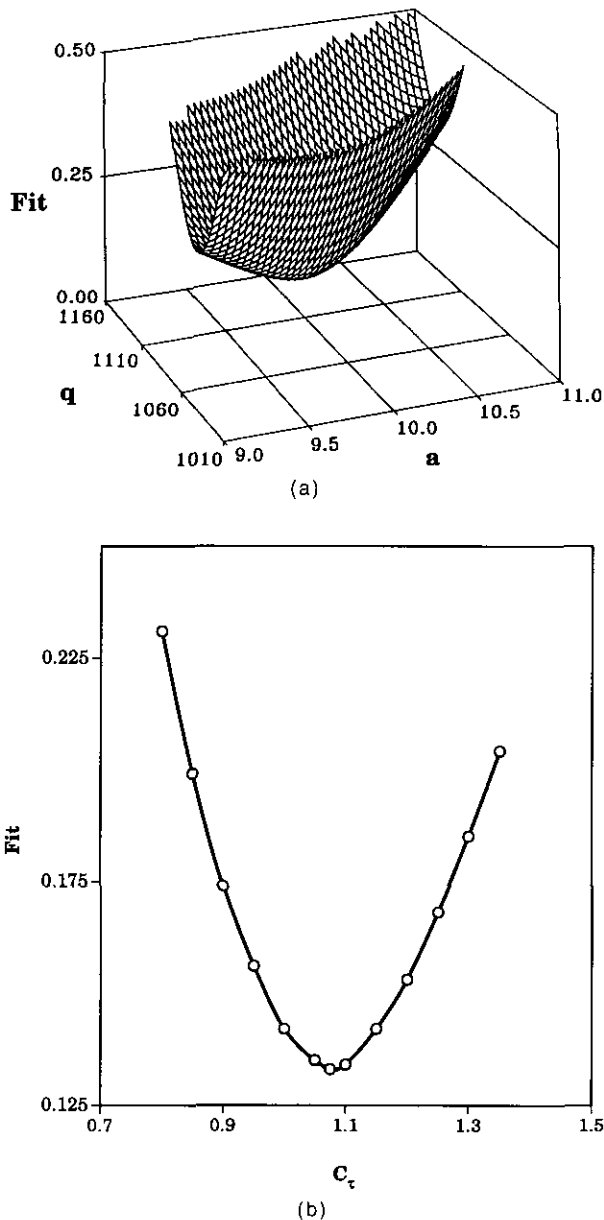


**Figure 3.** Determination of the energy parameters. (a) Three-dimensional plot of the fitting residual (r.m.s. standard deviation) as a joint function of  $a$  and  $q$ , at the optimal value of  $C_r$ . (b) Plot of the fitting residual (r.m.s. standard deviation) as a function of  $C_r$  (units of kcal/rad<sup>2</sup>) at the fixed optima of  $a$  and  $q$ .

ambiguous. An example is shown in Figure 3(a), which gives the r.m.s. deviation as a function of ( $a$ ,  $q$ ) for  $C_r = 0.747 \times 10^{-13}$  erg/rad<sup>2</sup> = 1.08 kcal/rad<sup>2</sup> at 50°C. This Figure shows the unique minimum found at this value of  $C_r$ . Next, a different value of  $C_r$  was specified, and the procedure was repeated. This was continued until the unique triplet of ( $q$ ,  $a$ ,  $C_r$ ) values giving the best fit to the data at the specified temperature was determined. Figure 3(b) shows the variation of the best fit at each  $C_r$  at 50°C and indicates the unique global minimum at this temperature. The minima in the residuals for all curve fittings were steep, as shown for the 50°C case in Figure 3(a). This means that the equilibrium values of the parameters could be determined with good precision.

The values of the free energy coefficients giving the best fit to the data at each temperature are listed in Table 1. It is clear that both  $q$  and  $C_r$  decrease with increasing temperature, while  $a$  is temperature-independent. The goodness-of-fit is expressed in the Table as the r.m.s. deviation between the observed and computed residual linking differences. The results of the fitting procedure are presented in Figure 4 as plots of the residual linking difference,  $\Delta Lk_r$ , versus  $\Delta Lk$ . The theoretical curves were calculated at each temperature using the optimal fit energy parameters (Table 1). Application of the  $\chi^2$  statistical test shows that the fit between the experimental results and the theoretical curves is significant at better than the 99.5% level.

(b) *Variation of the energy parameters with temperature*

The three energy parameters  $q$ ,  $a$  and  $C_r$  were each determined as a function of temperature. This enables us to calculate the corresponding enthalpy and entropy terms, according to the Gibbs-Helmholtz relationships. The Gibbs free energy of each of the processes dealt with in this analysis is:

$$\Delta G(T, P, \zeta) = \Delta H - T\Delta S, \quad (8a)$$

where  $\Delta H$  and  $\Delta S$  are the enthalpy and entropy changes involved,  $T$  is the absolute temperature,  $P$  is the pressure and  $\zeta$  represents the appropriate

**Table 1**  
*Best-fit values of the energy parameters as a function of temperature*

$T$ (°C)	$q$ (bp)	$C_r \times 10^{13}$ (erg rad <sup>-2</sup> )	$a$ (kcal/mol)	Fit†
40	1160	1.01	10.1	0.214
45	1125	0.868	10.5	0.154
50	1085	0.747	10.0	0.133
55	1035	0.66	10.1	0.227
60	973	0.469	10.4	0.223

† The r.m.s. deviation of the theoretical fitted curve from the experimental values.

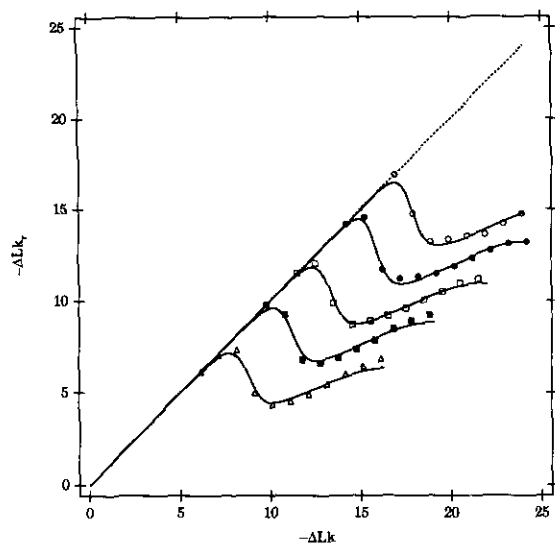


**Figure 4.** Plot of the residual linking number,  $\Delta Lk_r$ , versus the linking number,  $\Delta Lk$ , at temperatures of 60°C ( $\Delta$ ), 55°C ( $\blacksquare$ ), 50°C ( $\square$ ), 45°C ( $\bullet$ ) and 40°C ( $\circ$ ). The symbols in each case represent experimental points determined as described in Experimental Methods, and the continuous lines are the theoretical curves of best fit (minimum fitting standard deviation) at each temperature.

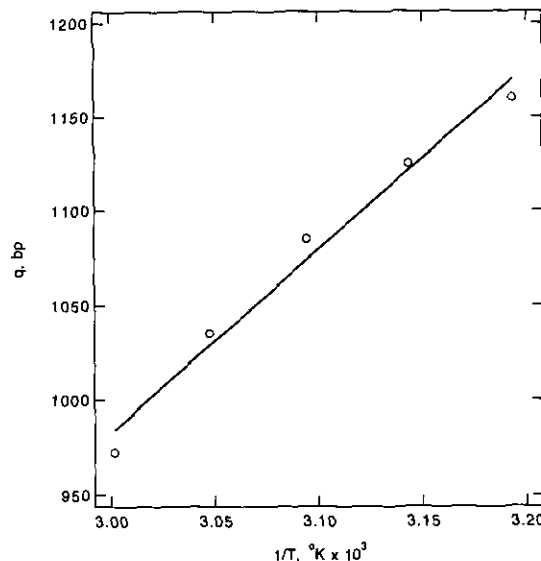


**Figure 5.** Plot of  $q(T) = NK(T)/RT$  versus  $1/T$ . The values of  $q(T)$  were taken from Table 1, and the continuous line is the best least-squares fit to the data.

force term, either  $\sigma$  or  $\tau$  (no force term is required for  $a$ ). The enthalpy and entropy are then given by:

$$\Delta H = \left[ \frac{\partial(\Delta G/T)}{\partial(1/T)} \right]_{P, \zeta} \quad (8b)$$

and:

$$\Delta S = - \left( \frac{\partial \Delta G}{\partial T} \right)_{P, \zeta} \quad (8c)$$

(i) *Topological state of the DNA*

The general expression for the free energy of a closed circular DNA of specified topological state was given in equation (6b) in terms of the specific linking difference,  $\sigma$ . Incorporating the definition  $K = RTq(T)/N$ , and using  $Lk_0 = N/h_0$ , the free energy expression becomes:

$$\Delta G(\sigma, T) = \frac{NRT}{h_0^2} q(T)\sigma^2. \quad (9)$$

This is conveniently written per base-pair (bp), with  $\Delta g \equiv \Delta G/N$ , as

$$\Delta g(\sigma, T) = \frac{RT}{h_0^2} q(T)\sigma^2. \quad (10)$$

The temperature dependence of the topological constraint free energy is shown in Figure 5, in which  $q(T) = NK/RT$  is plotted as a function of  $1/T$ . The data are well fit by a linear regression of the form:

$$q(T) = A/T + B. \quad (11)$$

Combining equations (10) and (11):

$$\Delta g(\sigma, T) = \frac{R\sigma^2}{h_0^2} (A + BT). \quad (12)$$

From equations (8b) and (8c), the supercoiling enthalpy and entropy (per bp) are both independent of temperature and are proportional to  $\sigma^2$ :

$$\Delta h(\sigma) = \frac{AR\sigma^2}{h_0^2} \quad (13a)$$

and:

$$\Delta s(\sigma) = \frac{-BR\sigma^2}{h_0^2}. \quad (13b)$$

The numerical results of the curve fitting are:

$$A = (0.968 \pm 0.077) \times 10^6 \text{ bp}^{-1}$$

$$B = -(1.92 \pm 0.28) \times 10^3 \text{ bp}^{-1} \text{ deg}^{-1},$$

with a regression coefficient of  $r^2 = 0.99$ .

Combining these numerical results with equations (13a) and (13b):

$$\Delta h(\sigma) = (17.5 \pm 1.7)\sigma^2 \text{ kcal/mol bp} \quad (14a)$$

$$\Delta s(\sigma) = (34.6 \pm 5.5)\sigma^2 \text{ cal/mol bp/deg.} \quad (14b)$$

At 37°C,  $T\Delta s = (10.7 \pm 1.7)\sigma^2$  kcal/mol bp, hence  $(T\Delta s)/\Delta h = 0.61 \pm 0.12$ . Also at 37°C, with the use of equation (12):

$$\Delta g(\sigma) = (6.8 \pm 1.2)\sigma^2 \text{ kcal/mol bp.} \quad (14c)$$

For a typical native plasmid DNA such as pBR322, having  $\langle \sigma \rangle = -0.054$ , hence  $\sigma^2 = 2.92 \times 10^{-3}$ , we find that  $\Delta h = 51(\pm 5)$  cal/mol bp and  $\Delta s = 0.10(\pm 0.02)$  cal/mol bp/deg. At 37°C,  $\Delta g = 20(\pm 3)$  cal/mol bp. The length of pBR322 DNA is  $N = 4363$  base-pairs, so for this molecule at



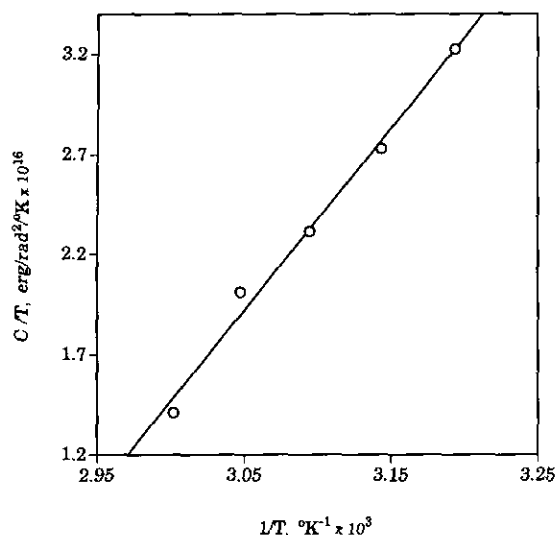


**Figure 6.** Plot of  $C_t/T$  versus  $1/T$ . The values of  $C_t$  were taken from Table 1, and the continuous line is the best least-squares fit to the data.

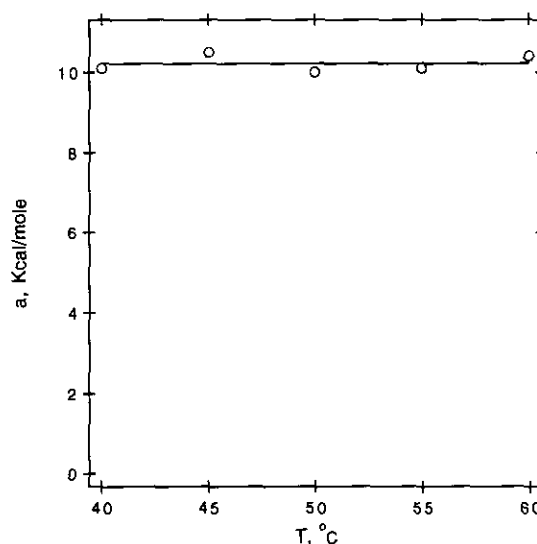


**Figure 7.** Plot of  $a$  versus  $T$ . The values of  $a$  were taken from Table 1. The continuous line is at constant  $a = 10.22$  kcal/mol.

the given linking difference we find  $\Delta H = 223(\pm 22)$  kcal/mol DNA and  $\Delta S = 0.44(\pm 0.07)$  kcal/mol DNA/deg. At  $37^\circ\text{C}$ ,  $T\Delta S = 136(\pm 22)$  kcal/mol DNA and  $\Delta G = 87(\pm 15)$  kcal/mol DNA.

#### (ii) Winding of denatured regions

The free energy of winding denatured regions is given by equation (7). The computed values of  $C_t(T)/T$  are plotted as a function of  $1/T$  in Figure 6 and are well fit by a straight line. The fitted curve is:

$$C_t/T = A_\tau/T + B_\tau, \quad (15)$$

with the coefficients:

$$A_\tau = (9.08 \pm 0.37) \times 10^{-13} \text{ erg/rad}^2, \\ \text{or } 13.1(\pm 0.5) \text{ kcal/rad}^2$$

$$B_\tau = -(0.0258 \pm 0.0011) \times 10^{-13} \text{ erg/rad}^2/\text{deg}, \\ \text{or } -37(\pm 2) \text{ cal/rad}^2/\text{deg}$$

and a regression coefficient of  $r^2 = 0.99$ .

Combining equation (15) with equations (8):

$$\Delta G(\tau, T) = \frac{n}{2} \tau^2 (A_\tau + B_\tau T) \quad (16a)$$

$$\Delta H(\tau) = (nA_\tau/2)\tau^2 \quad (16b)$$

$$\Delta S(\tau) = -(nB_\tau/2)\tau^2 \quad (16c)$$

$$T\Delta S(\tau)/\Delta H(\tau) = -B_\tau T/A_\tau \quad (16d)$$

We calculate from these numerical values that, at  $37^\circ\text{C}$ ,  $T\Delta S(\tau)/\Delta H(\tau) = 0.88 \pm 0.07$  and  $\Delta G(\tau, 37^\circ\text{C}) = 0.14 T\Delta S(\tau)$ .

#### (iii) Initiation of denaturation

The temperature variation of  $a$  is plotted in Figure 7. This parameter is independent of temperature at the 99% confidence level (Student's  $t$ ), with the result  $a = 10.22(\pm 0.67)$  kcal/mol.

## 5. Discussion

### (a) Local denaturation in closed circular DNA

In our previous studies of the temperature and  $\Delta Lk$ -dependent transitions of pSM1 DNA (Lee & Bauer, 1985), we proposed two alternative mechanisms to account for the accompanying reduction in twist: local denaturation and cruciform extrusion. Any other mechanism that reduces  $Tw$  is, of course, also possible. Fortunately, interpretation of the analogous transitions that we observe in pBR322 DNA is greatly simplified by the results of Kowalski and co-workers (Kowalski *et al.*, 1988), who showed that local denaturation is the only operative mechanism for pBR322 DNA at  $37^\circ\text{C}$ . Based upon mung bean nuclease digestion experiments,  $\Delta Lk$ -dependent denaturation occurs primarily in the region between nucleotides 3180 and 3301, a sequence that is 72% A + T.

Regarding the possibility of cruciform formation, pBR322 DNA contains three inverted repeats, as detected by  $S_1$  nuclease sensitivity (Lilley, 1980). The major and subminor inverted repeats are centered at 3065 and 3123 nucleotides and are 25 and 23 base-pairs in length, respectively. These both lie outside the region mapped by mung bean nuclease digestion and are too short to account for the transitions found in our experiments (see below). The minor inverted repeat is centered at 3221 nucleotides and is 26 base-pairs long. This sequence does lie within the mung bean nuclease mapped region, but its involvement is ruled out by the finding that several of the major mung bean sensitivity sites lie within the sequence in which the renatured arms of a putative minor cruciform would lie. In addition, stable cruciforms do not occur at low salt concentration when the temperature is above  $45^\circ\text{C}$  (Panyutin *et al.*, 1984). Denaturation that involves formation of a cruciform brings about

a change in twist that is numerically equal to  $-n/h_0$  and requires that  $\tau = 0$ . We find values of  $n \approx 45$  and  $\tau \approx -0.45$ , giving an actual change in  $Tw$  of about  $-6.2$ . By comparison, a cruciform that arose from the transition of 26 base-pairs would lead to a change in twist of only  $-2.6$ .

(b) *Thermodynamics of topologically constrained DNA*

The  $\Delta H$  and  $\Delta S$  values reported here were calculated from the Gibbs-Helmholtz relationships and exhibit little if any dependence upon temperature. For comparison, the enthalpy of native ColE1 *amp* plasmid closed circular DNA has been measured calorimetrically (Seidl & Hinz, 1984). The calorimetric result, at 37°C in a solution containing  $MgCl_2$ , was  $\Delta H = 2260$  kJ/mol DNA, or 540 kcal/mol DNA. These authors calculated a  $\Delta G$  of 921 kJ/mol DNA (220 kcal/mol DNA) from the Depew & Wang (1975) value of  $K$  and, by difference, obtained a  $\Delta S$  of 4.3 kJ/mol DNA per deg. (1.03 kcal/mol DNA per deg.). The ColE1 *amp* plasmid DNA used in the calorimetric experiments has length  $N = 10,900$  bp. Its specific linking difference was reported to be  $\sigma = -0.057$ . Using these constants, we calculate from our experimental results, equations (14), for the native ColE1 *amp* plasmid:

$$\Delta H = (620 \pm 60) \text{ kcal/mol DNA}$$

$$\Delta S = (1.23 \pm 0.20) \text{ kcal/mol DNA per deg.}$$

At 37°C:

$$\Delta G = (240 \pm 41) \text{ kcal/mol DNA.}$$

Considering the differences in the experimental conditions and methods, and that the comparison is between Gibbs-Helmholtz and calorimetric enthalpies, this agreement is indeed satisfactory.

In an alternative approach (Lee *et al.*, 1981), the temperature dependence of the unwinding of closed circular DNA by organic solvents was used to estimate a van't Hoff  $\Delta\Delta H$  of  $12.2 (\pm 0.4)$  kcal/mol DNA for a unit change in  $\Delta Lk$  for native pBR322 DNA. Using their measured value of  $\langle \Delta Lk \rangle = -22.4$ , their value of  $\Delta H$  for pBR322 is  $274 (\pm 9)$  kcal/mol DNA, compared to our calculation from equations (14) of  $223 (\pm 22)$  kcal/mol DNA. For the ColE1 *amp* plasmid, with  $\langle \Delta Lk \rangle = -59.2$ , the value obtained from the organic solvent results is  $722 (\pm 26)$  kcal/mol DNA. Our value of  $\Delta H = 620 (\pm 60)$  kcal/mol for this DNA is thus bracketed by the other two available  $\Delta H$  determinations.

A more direct confirmation of our results is found in a recent study of the helical repeat of DNA at elevated temperatures, using the Gaussian center method with the DNA ligase HB 8 from *Thermus thermophilus* (Duguet, 1993). This paper includes a plot (its Fig. 4) of a quantity related to the topological constraint energy coefficient *versus* temperature. Although the author presents no analysis of these data, we have used his published results to

construct a fit of  $q(T)$  *versus*  $1/T$ , obtaining a plot analogous to our Figure 5. This plot is an excellent straight line, having coefficients  $A_0 = (1.76 \pm 0.08) \times 10^6$  bp<sup>-1</sup> and  $B_0 = -(4.34 \pm 0.23) \times 10^3$  bp<sup>-1</sup> deg<sup>-1</sup>. (Here the subscripts are used to differentiate these estimates from our own, as well as to indicate that they refer to topoisomers in the vicinity of  $\Delta Lk = 0$ .) These coefficients are derived from experiments conducted in a solvent containing 30 mM Tris, 5 mM  $MgCl_2$  and 30 mM KCl. Numerically,  $A_0$  is approximately 70% larger than our  $A$  and  $B_0$  is about twice our  $B$ . The ratio of the  $T\Delta s_0/\Delta h_0$  terms is  $0.76 \pm 0.07$  at 37°C from the Gaussian center method, compared to our value of  $T\Delta s/\Delta h = 0.61 \pm 0.12$ . These ratios are indistinguishable at the 95% confidence level (Student's *t*). We consider the overall agreement to be satisfactory, considering that these two experimental series were conducted in quite different solvents, using closed DNAs of very different average  $\sigma$ . It is especially significant that the algebraic signs of both the  $\Delta H$  and the  $\Delta S$  calculated from the Gaussian center method data agree with our results. This point is discussed in greater detail in section (d) below.

(c) *Torsional rigidity of closed circular DNA*

The free energy coefficient associated with the topological constraint,  $K$ , can be written using equations (6c) and (11) as the sum of enthalpy and entropy contributions:

$$NK = NK_H + NK_S = RA + RBT. \quad (17)$$

At constant DNA length the enthalpy is equal to the elastic energy. It contains contributions from both bending and twisting, but the relative contributions have not been reliably determined by experiment. The torsional rigidity is defined in terms of the variance of the twist distribution,  $v_{Tw}$ , by:

$$C = \frac{NRT}{2\pi^2 N_A v_{Tw}}, \quad (18)$$

where  $v_{Tw} = RT/K_{Tw}$ ,  $N_A$  is Avogadro's number, and  $l = 3.36$  Å is the separation between adjoining base-pairs in the B-form DNA duplex. Now  $K_H \leq K_{Tw}$ , with the difference depending upon the relative contribution from the bending energy. The use of  $K_H$  for  $K_{Tw}$  overestimates  $v_{Tw}$ , hence underestimates  $C$ . If we neglect any bending contribution to the elastic energy (here  $\Delta H$ ), and use  $K_H$  to estimate  $K_{Tw}$ , then  $C$  is estimated by  $C_H$ , given by (Barkley & Zimm, 1979):

$$C_H = \frac{NK_H l}{2\pi^2 N_A} = \frac{RA l}{2\pi^2 N_A}, \quad (19)$$

where  $R = 4.186 \times 10^7$  erg/mol. Equation (19), with our value of  $A$ , leads to a lower limit of  $C_H = (2.3 \pm 0.2) \times 10^{19}$  erg cm. This is very close to the estimates of  $C = 2.9 \times 10^{19}$  erg cm (Horowitz & Wang, 1984) and  $2.4 \times 10^{19}$  erg cm (Shore & Baldwin, 1983) obtained from measurements on

very small DNA circles. Monte Carlo calculations using small DNA rings suggest that writhe (bending) fluctuations contribute about 20% to the difference between  $K_H$  and  $K_{Tw}$  (Crothers *et al.*, 1992; Levene & Crothers, 1986). This theoretical result was used to correct the  $C = 2.9 \times 10^{-19}$  measurement (Horowitz & Wang, 1984) to  $C = 3.4 \times 10^{-19}$  erg cm for twist alone. Calculations based upon a continuous elastic model of DNA (Hunt & Hearst, 1991) also suggest that the twist contributions should dominate the total elastic energy (in the absence of entropy considerations) at low salt and moderate  $\sigma$ , although not to the complete exclusion of bending. The close agreement between our result and those with small DNA rings suggests the possibility that the  $\Delta h$  term is insensitive to DNA length, while the  $\Delta s$  term decreases as the DNA becomes smaller.

As calculated from  $\Delta H$ , the apparent torsional rigidity shows no significant dependence upon temperature over the range examined. This does not preclude a temperature-dependent interconversion between torsional and bending energy. If such an interconversion occurs, the actual torsional rigidity might show temperature dependence even with constant  $\Delta H$ .

#### (d) Topological constraint entropy

We determine that the entropy of topologically constrained closed circular DNA is positive and varies with  $\sigma^2$  (refer to eqn (14b) and the accompanying text). This is in agreement with previous estimates of  $\Delta S$  made from calorimetric (Seidl & Hinz, 1984) and van't Hoff (Lee *et al.*, 1981) measurements of  $\Delta H$ . A positive entropy was also obtained from our analysis of the experimental results of Duguet, which were found by a Gaussian center fitting to distributions of topoisomers over a temperature range of 35°C to 85°C (Duguet, 1993). All available experimental results are thus in agreement concerning both the sign and the approximate magnitude of the entropy of supercoiling.

Monte Carlo calculations of the chain configuration entropy of topologically constrained DNA have been performed (Vologodskii *et al.*, 1992), based upon a cylindrical polygon representation of the DNA duplex from which twist fluctuations were excluded. The calculated chain configuration entropy found by this procedure is negative. This accords with the expectation that the formation of supercoils constitutes a restraint upon the number of degrees of freedom of the chain. The chain configuration entropy cannot, however, be used alone to predict the experimental entropy, since the actual net entropy change upon supercoiling involves several additional factors. These include  $\Delta Lk$ -dependent changes in local interactions between base-pairs, changes in base-pair-solvent interactions, and changes in solvent structure. Comparison between the experimental and the Monte-Carlo results shows that non-chain configuration contributions to the topological constraint

entropy are large and positive. In fact, they clearly dominate the entropy change under all experimental conditions examined to date. It is clear that extreme caution is required in using the results of Monte Carlo and other statistical calculations to make predictions concerning the actual behavior of closed circular DNA in solution.

#### (e) Interstrand winding of denatured regions in closed circular DNA

The denaturation of an internal region of duplex DNA proceeds in two stages. First, the weak interactions responsible for local duplex stability (stacking interactions, hydrogen bonds, etc.) are disrupted, and the local winding number is reduced from  $+n/h_0$  to 0. Second, the denatured strands intertwine to an extent determined by the net torsional forces. In a topologically constrained DNA of negative  $\Delta Lk$ , the net torsion on the duplex produces left-handed (–) winding. This is reflected in two energy terms: the entropy is expected to change relative to unconstrained single strands, and the forced proximity of the bases will favor chemical interactions that will be expressed in the enthalpy. The force constant associated with interstrand twisting of denatured DNA strands determines the free energy of these interactions, and its temperature dependence determines the corresponding  $\Delta S$  and  $\Delta H$ .

A value  $C_\tau = 1.8 \times 10^{-13}$  erg rad<sup>-2</sup> was estimated from a theoretical analysis (Crothers & Spatz, 1971) of the unwinding kinetics of T2 DNA, determined in alkali at 0.4 M NaCl and 30°C (Spatz & Crothers, 1969). The authors state that the value of  $C_\tau$  (for which they used the symbol  $b$ ) is independent of ionic strength above 0.4 M NaCl but increases at low salt by an unspecified amount. Extrapolating our results (Fig. 6) to 30°C gives the estimate that  $C_\tau = (1.3 \pm 0.1)$  erg rad<sup>-2</sup> in low salt at pH 8.4. Direct comparison of our estimate of  $C_\tau$  with that determined by Crothers & Spatz (1971) is complicated by the unusual structural features of T2 DNA (Lehman & Pratt, 1960), which contains hydroxymethylcytosine (75% glucosylated) in place of cytosine. These modifications are expected to increase the free energy of winding the denatured strands, which should in turn increase  $C_\tau$ . The value that we report here refers to unmodified DNA.

Having measured the temperature dependence of  $C_\tau$ , we have obtained first determinations of the enthalpy and entropy of the winding of denatured strands. We find that the free energy  $\Delta g_\tau$  for the transfer of one base-pair from unwound coil to an intertwined structure having helicity of  $\tau$  radians per base-pair, is positive at room temperature and decreases with increasing temperature. An effective  $T_{m,\tau}$  may be defined for this process as the temperature at which  $\Delta g_\tau = 0$ , giving  $T_{m,\tau} = 78^\circ\text{C}$ . The entropy change for this process is positive, even though a naive analysis would suggest that the configuration entropy for interstrand winding should be negative. Again, solvent effects appear to

dominate this entropy change. The enthalpy of this process is likewise difficult to interpret, since it includes contributions both from the interaction of the bases on opposite strands and from changes in water-water and water-base interactions. We expect  $\Delta h$  to be a strong function of the ionic strength, and it might depend upon base composition as well.

#### (f) Initiation of denaturation

We determine that the factor  $a$ , associated with the initiation of denaturation of a run of  $n$  base-pairs, is independent of temperature and equal to  $10.2(\pm 0.7)$  kcal/mol. This experimental result can be interpreted as including contributions from both unstacking of the first base-pair and from the entropy of forming a loop of  $n$  base-pairs. No good theory is available to calculate this latter factor at low  $n$ , but it can be estimated from the Jacobson-Stockmayer (Jacobson & Stockmayer, 1950) formulation at values of  $n \geq 30$  to 40. Following Zimm (1960), we combine these factors in the form  $\xi = \xi_0(1+n)^{-3/2}$ , where the unstacking contribution to the initiation of denaturation is  $\Delta G_{i,st} = -RT \ln \xi_0$  and the free energy of loop formation is  $(3/2)RT \ln(1+n)$ . Then the free energy of initiation of melting is  $a = -RT \ln \xi = -RT \ln \xi_0 + (3/2)RT \ln(1+n)$ . The unstacking contribution to the free energy is then  $\Delta G_{i,st} = a - (3/2)RT \ln(1+n)$ . For values of  $n$  over the narrow range 40 to 50 base-pairs, as occur in our experiments, the logarithmic term varies weakly with  $n$  and has values between  $5.6 RT$  and  $5.8 RT$ . At  $30^\circ\text{C}$ , where  $RT = 0.602$  kcal/mol, this term is approximately 3.4 kcal/mol. We therefore estimate that  $\Delta G_{i,st} \approx 6.8$  kcal/mol. This value is comparable to estimates by others (Amirikyan *et al.*, 1981; Benham, 1992; Crothers & Zimm, 1964).

We acknowledge the technical expertise of Ms Beth Lin, who was responsible for DNA preparation and the gel electrophoresis. This research was supported by separate grants from the NIH to W.R.B. and to C.J.B.

#### References

- Adrian, M., ten Heggeler-Bordier, B., Wahli, W., Stasiak, A. Z., Stasiak, A. & Dubochet, J. (1990). Direct visualization of supercoiled DNA molecules in solution. *EMBO J.* **9**, 4551–4554.
- Amirikyan, B. R., Vologodskii, A. V. & Lyubchenko, Y. L. (1981). Determination of DNA cooperativity factor. *Nucl. Acids Res.* **9**, 5469–5482.
- Barkley, M. D. & Zimm, B. H. (1979). Theory of twisting and bending of chain macromolecules: analysis of the fluorescence depolarization of DNA. *J. Chem. Phys.* **70**, 2991–3007.
- Bauer, W. R. (1978). Structure and reactions of closed duplex DNA. *Annu. Rev. Biophys. Bioeng.* **7**, 287–313.
- Bauer, W. R. & Gallo, R. (1989). Physical and topological properties of closed circular DNA. In *Chromosomes: Eukaryotic, Prokaryotic, and Viral* (Adolph, K. W., ed.), pp. 87–126. CRC Press, Boca Raton, FL.
- Bauer, W. & Vinograd, J. (1970). Interaction of closed circular DNA with intercalative dyes. II. The free energy of superhelix formation in SV40 DNA. *J. Mol. Biol.* **47**, 419–435.
- Benham, C. J. (1990). Theoretical analysis of heteropolymeric transitions in superhelical DNA molecules of specified sequence. *J. Chem. Phys.* **92**, 6294–6305.
- Benham, C. J. (1992). Energetics of the strand separation transition in superhelical DNA. *J. Mol. Biol.* **225**, 835–847.
- Benjamin, H. W. & Cozzarelli, N. R. (1985). DNA-directed synapsis in recombination: slithering and random collision of sites. In *Genetic Chemistry: The Molecular Basis of Heredity*, pp. 107–129. The Robert A. Welch Foundation, Houston, TX.
- Bliska, J. B. & Cozzarelli, N. R. (1987). Use of site-specific recombination as a probe of DNA structure and metabolism *in vivo*. *J. Mol. Biol.* **194**, 205–218.
- Boles, T. C., White, J. H. & Cozzarelli, N. R. (1990). Structure of plectonemically supercoiled DNA. *J. Mol. Biol.* **213**, 931–951.
- Breslauer, K. J., Frank, R., Blöcker, H. & Marky, L. A. (1986). Predicting DNA duplex stability from the base sequence. *Proc. Nat. Acad. Sci., U.S.A.* **83**, 3746–3750.
- Crothers, D. M. & Spatz, H. C. (1971). Theory of friction-limited DNA unwinding. *Biopolymers*, **10**, 1949–1972.
- Crothers, D. M. & Zimm, B. H. (1964). Theory of the melting transition of synthetic polynucleotides: evaluation of the stacking free energy. *J. Mol. Biol.* **9**, 1–9.
- Crothers, D. M., Drak, J., Kahn, J. D. & Levene, S. D. (1992). DNA bending, flexibility, and helical repeat by cyclization kinetics. In *Methods in Enzymology* (Lilley, D. M. J. & Dahlberg, J. E., eds), vol. 212, pp. 3–29. Academic Press, Inc., New York.
- Depew, R. E. & Wang, J. C. (1975). Conformational fluctuations of DNA helix. *Proc. Nat. Acad. Sci., U.S.A.* **72**, 4275–4279.
- Duguet, M. (1993). The helical repeat of DNA at high temperature. *Nucl. Acids Res.* **21**, 463–468.
- Hagerman, P. J. (1988). Flexibility of DNA. *Annu. Rev. Biophys. Chem.* **17**, 265–286.
- Horowitz, D. S. & Wang, J. C. (1984). Torsional rigidity of DNA and length dependence of the free energy of DNA supercoiling. *J. Mol. Biol.* **173**, 75–91.
- Hunt, N. G. & Hearst, J. E. (1991). Elastic model of DNA supercoiling in the infinite-length limit. *J. Chem. Phys.* **95**, 9329–9336.
- Jacobson, H. & Stockmayer, W. (1950). Intramolecular reaction in polycondensations. I. The theory of linear systems. *J. Chem. Phys.* **18**, 1600–1606.
- Klysik, J., Rippe, K. & Jovin, T. M. (1991). Parallel-stranded DNA under topological stress: rearrangement of  $(dA)_{15} \cdot (dT)_{15}$  to a  $d(A \cdot A \cdot T)_n$  triplex. *Nucl. Acids Res.* **19**, 7145–7154.
- Kowalski, D., Natale, D. A. & Eddy, M. J. (1988). Stable DNA unwinding, not “breathing”, accounts for single-strand-specific nuclease hypersensitivity of specific A+T-rich sequences. *Proc. Nat. Acad. Sci., U.S.A.* **85**, 9464–9468.
- Lee, C. H., Mizusawa, H. & Kakefuda, T. (1981). Unwinding of double-stranded DNA helix by dehydration. *Proc. Nat. Acad. Sci., U.S.A.* **78**, 2838–2842.
- Lee, F. S. & Bauer, W. R. (1985). Temperature dependence of the gel electrophoretic mobility of superhelical DNA. *Nucl. Acids Res.* **13**, 1665–1682.
- Lehman, I. R. & Pratt, E. A. (1960). On the structure of

- the glucosylated hydroxymethylcytosine nucleotides of coliphages T2, T4 and T6. *J. Biol. Chem.* **235**, 3254–3259.
- Levene, S. D. & Crothers, D. M. (1986). Topological distributions and the torsional rigidity of DNA. A Monte Carlo study of DNA circles. *J. Mol. Biol.* **189**, 73–83.
- Lilley, D. M. (1980). The inverted repeat as a recognizable structural feature in supercoiled DNA molecules. *Proc. Nat. Acad. Sci., U.S.A.* **77**, 6468–6472.
- Lilley, D. M. J. (1987). The structure and physical chemistry of cruciform structures in supercoiled DNA. In *Structure and Dynamics of Biopolymers* (Nicolini, C., ed.), pp. 112–136, Martinus Nijhoff, Dordrecht.
- Lobell, R. B. & Schleif, R. F. (1990). DNA looping and unlooping by AraC protein. *Science*, **250**, 528–532.
- Manning, G. S. (1988). Three persistence lengths for a stiff polymer with an application to DNA B-Z junctions. *Biopolymers*, **27**, 1529–1542.
- Marmur, J. & Doty, P. (1962). Determination of the base composition of deoxyribonucleic acid from its thermal denaturation temperature. *J. Mol. Biol.* **5**, 109–118.
- Nordheim, A., Peck, L. J., Lafer, E. M., Stollar, B. D., Wang, J. C. & Rich, A. (1983). Supercoiling and left-handed Z-DNA. *Cold Spring Harbor Symp. Quant. Biol.* **47**, 93–100.
- Panyutin, I., Klishko, V. & Lyamichev, V. (1984). Kinetics of cruciform formation and stability of cruciform structure in superhelical DNA. *J. Biomol. Struct. Dynam.* **1**, 1311–1324.
- Pulleyblank, D. E., Shure, M., Tang, D., Vinograd, J. & Vosberg, H. P. (1975). Action of nicking-closing enzyme on supercoiled and nonsupercoiled closed circular DNA: formation of a Boltzmann distribution of topological isomers. *Proc. Nat. Acad. Sci., U.S.A.* **72**, 4280–4284.
- Rhodes, D. & Klug, A. (1980). Helical periodicity of DNA determined by enzyme digestion. *Nature (London)*, **287**, 573–578.
- Sambrook, J., Fritsch, E. F. & Maniatis, T. (1989). *Molecular Cloning: A Laboratory Manual* (2nd Edit.), Cold Spring Harbor Laboratory Press, Cold Spring Harbor, NY.
- Schildkraut, C. & Lifson, S. (1965). Dependence of the melting temperature of DNA on salt concentration. *Biopolymers*, **3**, 195–208.
- Schleif, R. (1988). DNA looping. *Science*, **24**, 127–128.
- Seidl, A. & Hinz, H.-J. (1984). The free energy of DNA supercoiling is enthalpy-determined. *Proc. Nat. Acad. Sci., U.S.A.* **81**, 1312–1316.
- Shore, D. & Baldwin, R. L. (1983). Energetics of DNA twisting. I. Relation between twist and cyclization probability. *J. Mol. Biol.* **170**, 957–981.
- Sinden, R. R. & Pettijohn, D. E. (1982). Torsional tension in intracellular bacteriophage T4 DNA. Evidence that a linear DNA duplex can be supercoiled *in vivo*. *J. Mol. Biol.* **162**, 659–677.
- Sinden, R. R., Carlson, J. O. & Pettijohn, D. E. (1980). Torsional tension in the DNA double helix measured with trimethylpsoralen in living *E. coli* cells: analogous measurements in insect and human cells. *Cell*, **21**, 773–783.
- Spatz, H. C. & Crothers, D. M. (1969). The rate of DNA unwinding. *J. Mol. Biol.* **42**, 191–219.
- Vinograd, J. & Lebowitz, J. (1966). Physical and topological properties of circular DNA. *J. Gen. Physiol.* **49**, 103–125.
- Vologodskii, A. V., Levene, S. D., Klenin, K. V., Frank-Kamenetskii, M. & Cozzarelli, N. R. (1992). Conformational and thermodynamic properties of supercoiled DNA. *J. Mol. Biol.* **227**, 1224–1243.
- Wang, J. C. (1979). Helical repeat of DNA in solution. *Proc. Nat. Acad. Sci., U.S.A.* **76**, 200–203.
- White, J. H. (1969). Self-linking and the Gauss integral in higher dimensions. *Amer. J. Math.* **91**, 693–728.
- White, J. H. (1989). An introduction to the geometry and topology of DNA structure. In *Mathematical Methods for DNA Sequences* (Waterman, M. S., ed.), pp. 225–253, CRC Press, Inc., Boca Raton, FL.
- White, J. H., Cozzarelli, N. R. & Bauer, W. R. (1988). Helical repeat and linking number of surface wrapped DNA. *Science*, **241**, 323–327.
- Zimm, B. H. (1960). Theory of “melting” of the helical form in double chains of the DNA type. *J. Chem. Phys.* **33**, 1349–1356.